Supporting Information

Structure-Induced Partial Phase Transformation Endow Hollow TiO_2/TiN Heterostructure Fibers Stacked by Nanosheets Arrays with Extraordinary Sodium Storage Performance

Pan Xue[a]‡, Qiulong Li[a, d]‡, Wenbin Gong[c]‡, Zhongti Sun[b], Han Wang[a], Kaiping Zhu[a], Can Guo[a], Guo Hong[f, g]*, Weigao Xu[h], Jingyu Sun[b], Yagang Yao[a]*, Zhongfan Liu[b, e]

a. National Laboratory of Solid State Microstructures, College of Engineering and Applied Sciences, Nanjing University, Nanjing 210093, China

b. College of Energy, Soochow Institute for Energy and Materials Innovations (SIEMIS), Key Laboratory of Advanced Carbon Materials and Wearable Energy, Technologies of Jiangsu Province, Soochow University, Suzhou 215006, China

c. School of Physics and Energy, Xuzhou University of Technology, Xuzhou 221018, China

d. College of Materials Science and Engineering, Nanjing Tech University, 30 Puzhu Road, Nanjing 211816, China

e. Center for Nanochemistry (CNC), College of Chemistry and Molecular Engineering, Peking University, Beijing 100871, China

f. Institute of Applied Physics and Materials Engineering, University of Macau. Avenida da Universidade, Taipa, Macau SAR 999078, China

g. Department of Physics and Chemistry, Faculty of Science and Technology, University of Macau, Avenida da Universidade, Taipa, Macau SAR 999078, China

h. Key Laboratory of Mesoscopic Chemistry, School of Chemistry and Chemical Engineering, Nanjing University, Nanjing 210093, China

[*] Email: ygyao2018@nju.edu.cn (Y. Yao); ghong@um.edu.mo (G. Hong)

Raw Materials

1M sodium perchlorate ($NaClO_4$) dissolved in propylene carbonate (PC) and ethylene carbonate (EC) (1:1, v/v were obtained from dodochem Co., Ltd.), and which was added 5% fluoroethylene carbonate (FEC). Glass fibers (Whatman) were selected as separators. All materials were stored and handled in an mikrouna glove box under Ar atmosphere (<0.01 ppm H_2O and <0.01 ppm O_2). Polyvinyl pyrrolidone （PVP, M ≈ 1.3 M）, anhydrous ethanol (EtOH, 99%), anhydrous acetate acid (HAc, 99%) and tetrabutyl titanate（TNB, 99%）were sourced from Shanghai Aladdin Biochemical Technology Co., Ltd. Cu foils were purchased from Hefei Kejing Material Technology Co., Ltd.

Characterization

Morphological and structural characterizations were conducted using a Hitachi 4800 SEM. XRD spectra were obtained from a Bruker-D8 ADVANCE X-ray diffractometer. High‐resolution transmission electron microscopy (HRTEM) and energy dispersive X‐ray (EDX) elemental mapping images were acquired by a FEI TEC‐NAI G220 high resolution TEM (200 kV). XPS analysis was performed using an ESCALAB 250Xi system from Thermo Scientific. The nitrogen adsorption-desorption isotherms were demonstrated using a Quantachrome Autosorb-IQ2 at 77 K. Specific surface areas were illustrated by Brunauer-Emmett-Teller analysis.

Experimental Section

Preparation of TiO_2: The precursor fibers were prepared by electrospinning solutions of PVP/HAc/EtOH/TNB. Specifically, PVP powder (1.5 g) and TNB (5 g) were added into the mixed solvent of EtOH/HAc (11 g/1 g) and stirred for 4 h until a yellow precursor solution was obtained. The solution was injected into a syringe with a stainless steel spinneret (18 G), with a voltage of 18-20 kV applied to the spinneret. The distance between the stainless steel spinneret and flat receiver

was 20 cm. The fiber samples were collected on Al foil, dried for 12 h at 30 °C in air, and then annealed at 320 °C for 6 h under air atmosphere at a rate of 5 °C min^{-1}. The pure TiO_2 were synthesized by using a simple hydrothermal reaction under weak alkaline conditions. Generally, 80 mg of amorphous TiO_2 fibers were immersed in 1 M NaOH aqueous solution and transferred into a stainless steel autoclave lined with Teflon, with a total volume of 40 mL, and then the autoclave was at 150 °C for 36 h. The product was washed repeatedly with deionized water and adjusted to pH = 7 with 0.1 M HCl. Then the product was collected, dried, and calcined at 550 °C for 2 h.

Preparation of HTTFs: High-purity Ar (rate: 200 sccm) and NH_3 (rate:100 sccm) were used as protective gas and reagent gas. Annealing of pure TiO_2 for 0.5-12 h is marked as HTTFs-0.5h, HTTFs-1h, HTTFs-2h and pure TiN, respectively.

DFT calculations: The electronic properties of HTTFs were calculated at the density functional theory (DFT) level as implemented in the Vienna ab initio simulation package (VASP), using the projector-augmented wave (PAW) potentials with a plane-wave cutoff of 500 eV. The Perdew Burke Ernzerhof (PBE) form of the exchange correlations functional was employed in the simulation, and the long-range interlayer van der Waal s (vdW) interaction was described with DFT-D2 method. The HTTFs was modeled as the interface consisting of TiO_2 and TiN in this study. The structure of HTTFs was optimized by using the conjugate gradient method, in which the convergence for total energy and interaction force was set to be 10^{-6} eV and 10^{-3} eV/Å, respectively. The climbing nudged elastic band (cNEB) method was employed to calculate the reaction barrier with the force tolerance of 5×10^{-2} eV/Å.

Electrochemical measurements: CV and EIS for the as-prepared samples were obtained using an electrochemical workstation (CHI 760E). For EIS measurements, an amplitude of 5 mV and a frequency range between 10 mHz and 100 kHz was applied to the cells.

The electrochemical performances of all samples were evaluated in CR2032 half-cells with Na metal as the counter electrode/reference electrode. HTTFs electrodes were fabricated by mixing HTTFs, super-p, and binder polyvinylidene fluoride with a mass ratio of 7:2:1. The electrolyte is 1 M $NaClO_4$ dissolved in a mixed solution of ethylene carbonate (EC) and propylene carbonate (PC) (1:1, v/v) and added with 5% fluoroethylene carbonate (FEC) as additive. Glass fiber (Whatman) was selected as the separator. The cut-off potentials of charge and discharge were set at 3.0 and 0.01 V (vs. Na^+/Na).

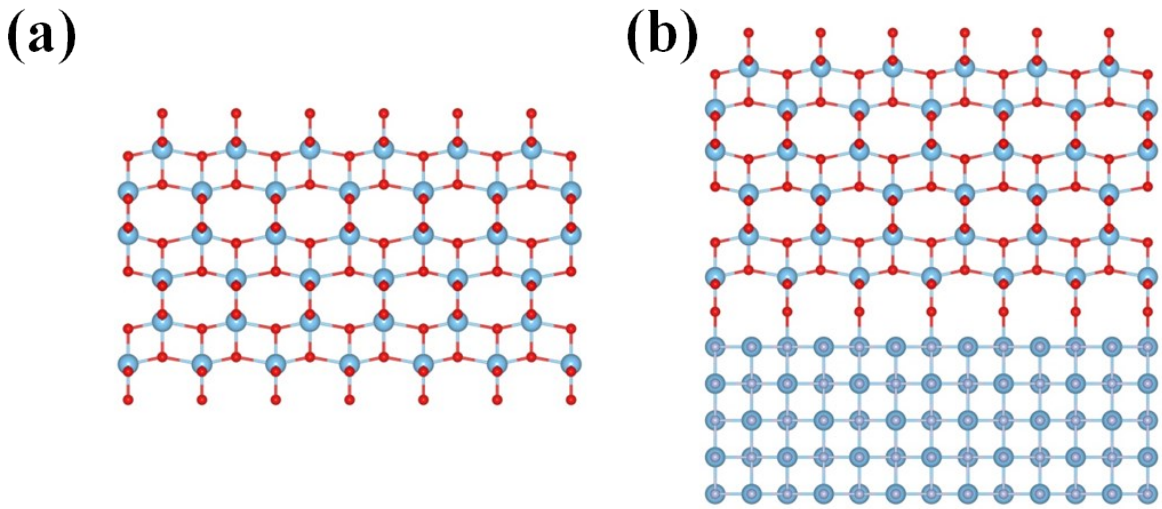

Fig. S1 Structures of (a) TiO_2 and (b) TiO_2/TiN interface of HTFFs. Gray, red, and blue ball marks N, O, and Ti atom, respectively.

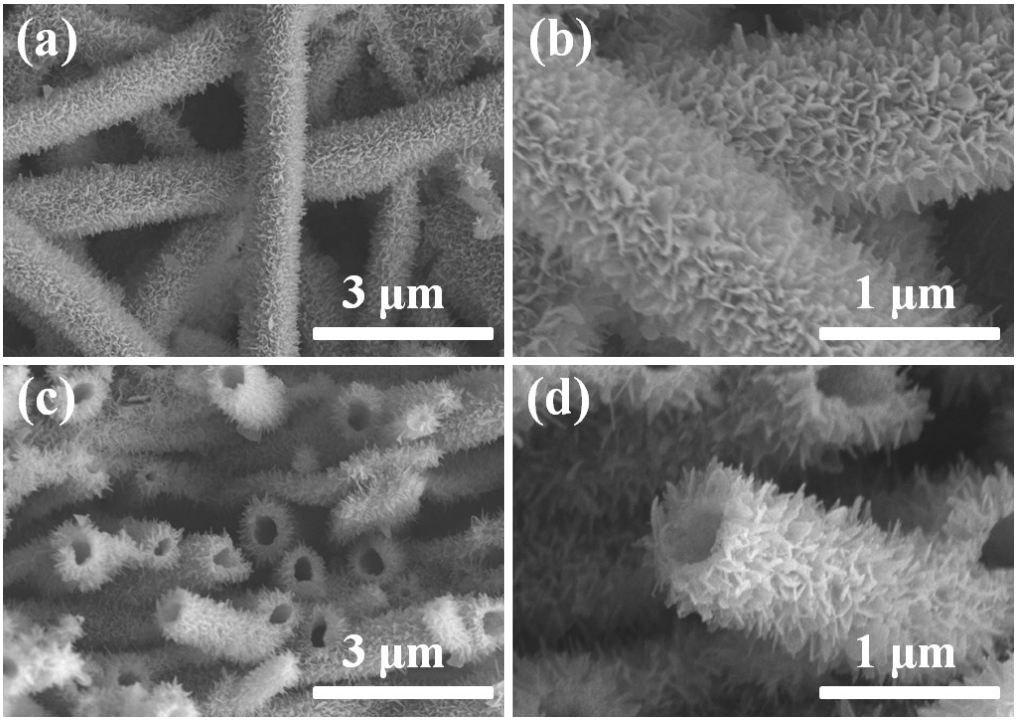

Fig. S2 (a,b) Top-view SEM images of the top surface of the pure TiO_2. (c,d) Cross-sectional SEM images showing pure TiO_2 hosts with a fiber diameter of 750 nm.

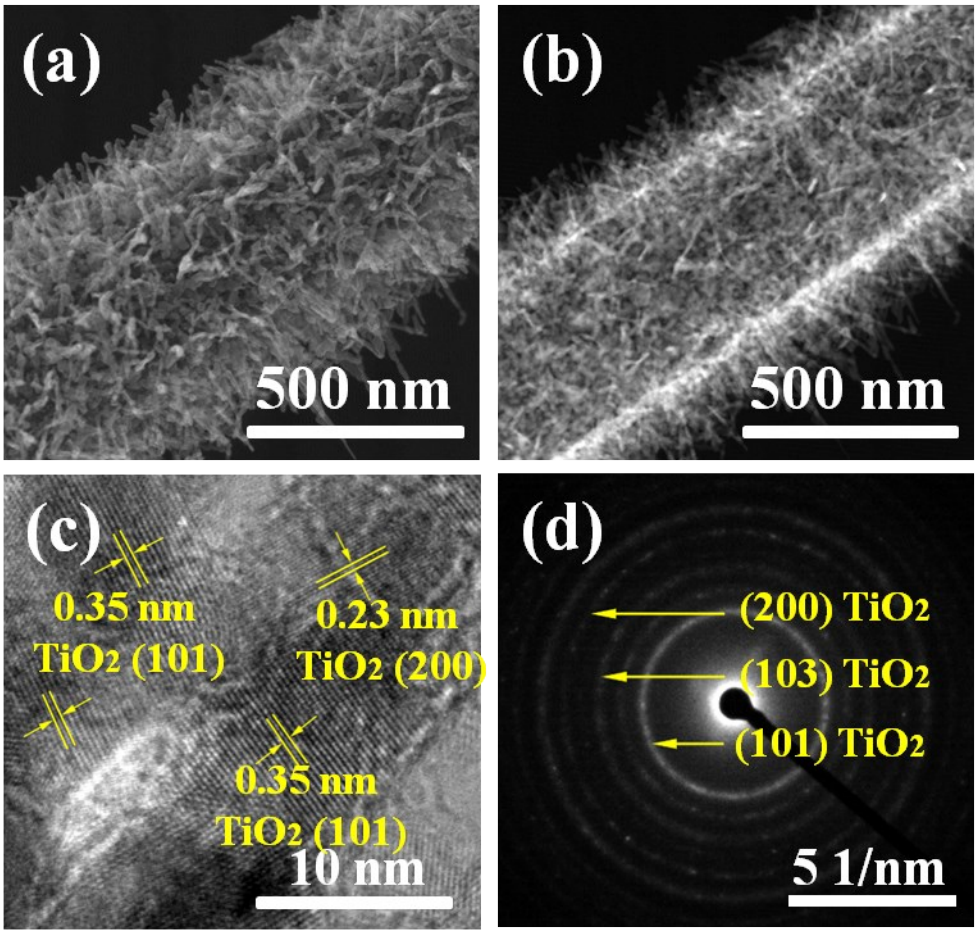

Fig. S3 (a,b) TEM, (c) HRTEM and (d) selected-area electron diffraction images of the pure TiO_2.

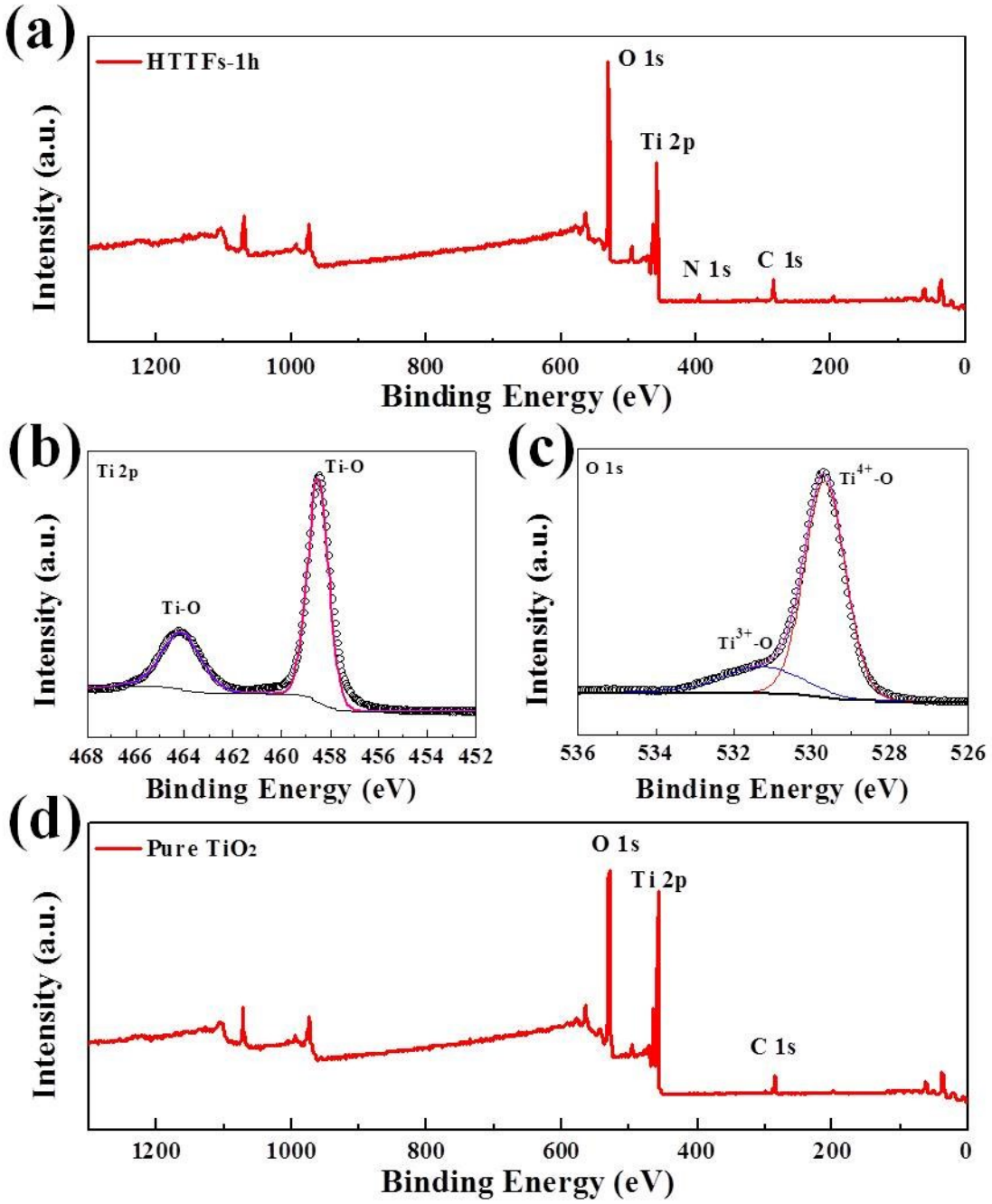

Fig. S4 XPS characterization of the (a) HTTFs-1h and (d) pure TiO_2, core-level spectra of (b) Ti 2p and (c) O 1s peaks of pure TiO_2.

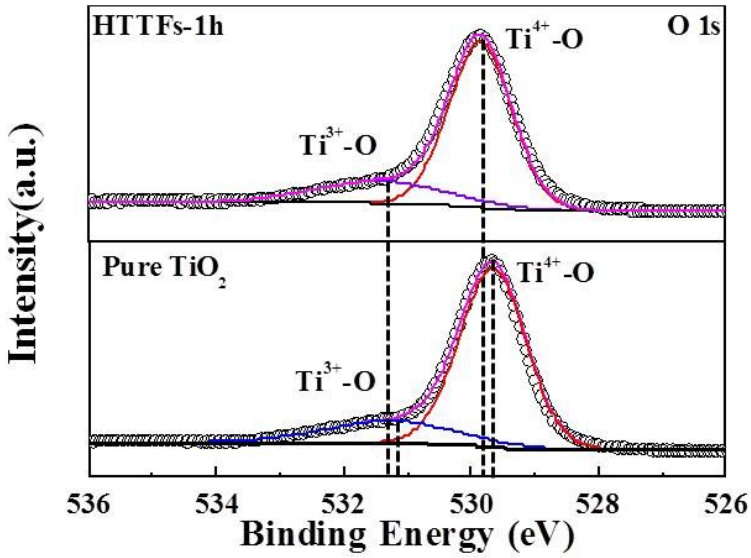

Fig. S5 High-resolution XPS spectra of O 1s for HTTFs-1h and pure TiO_2.

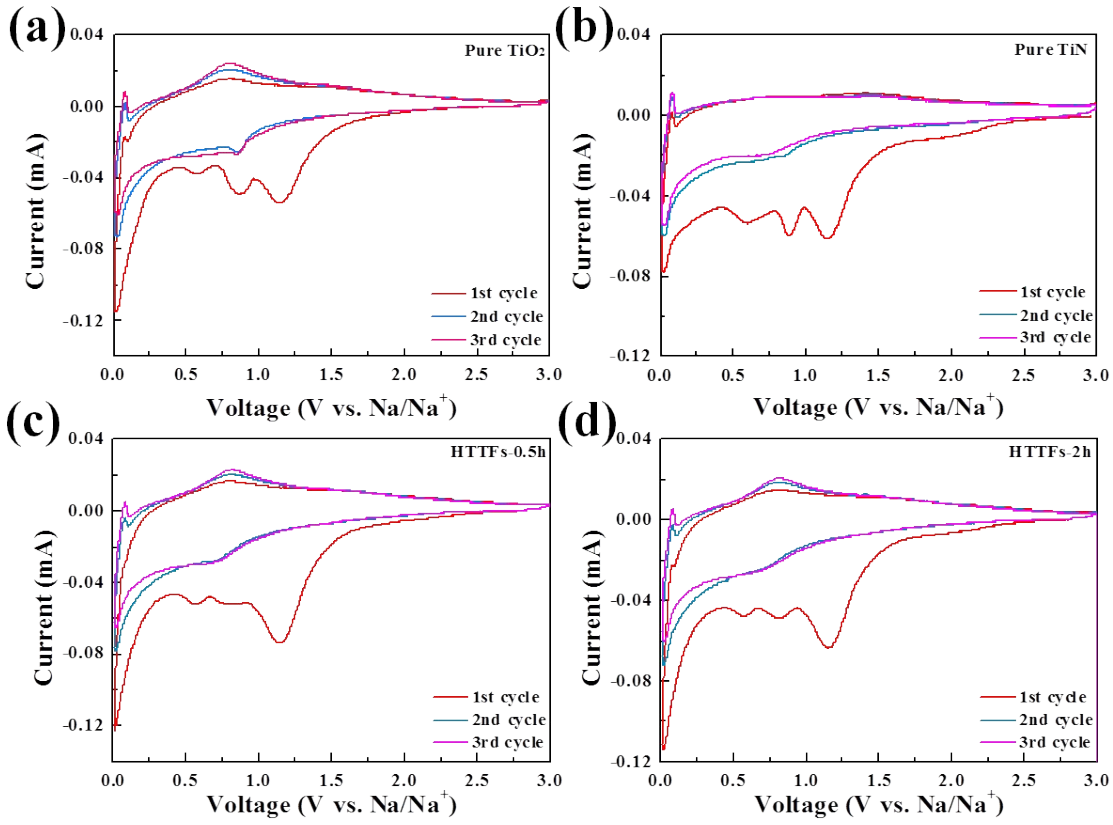

Fig. S6 Cyclic voltammograms for the first 3 cycles of pure TiO_2, pure TiN, HTTFs-0.5h and HTTFs-2h with a scan rate of 0.1 mV s^{-1}.

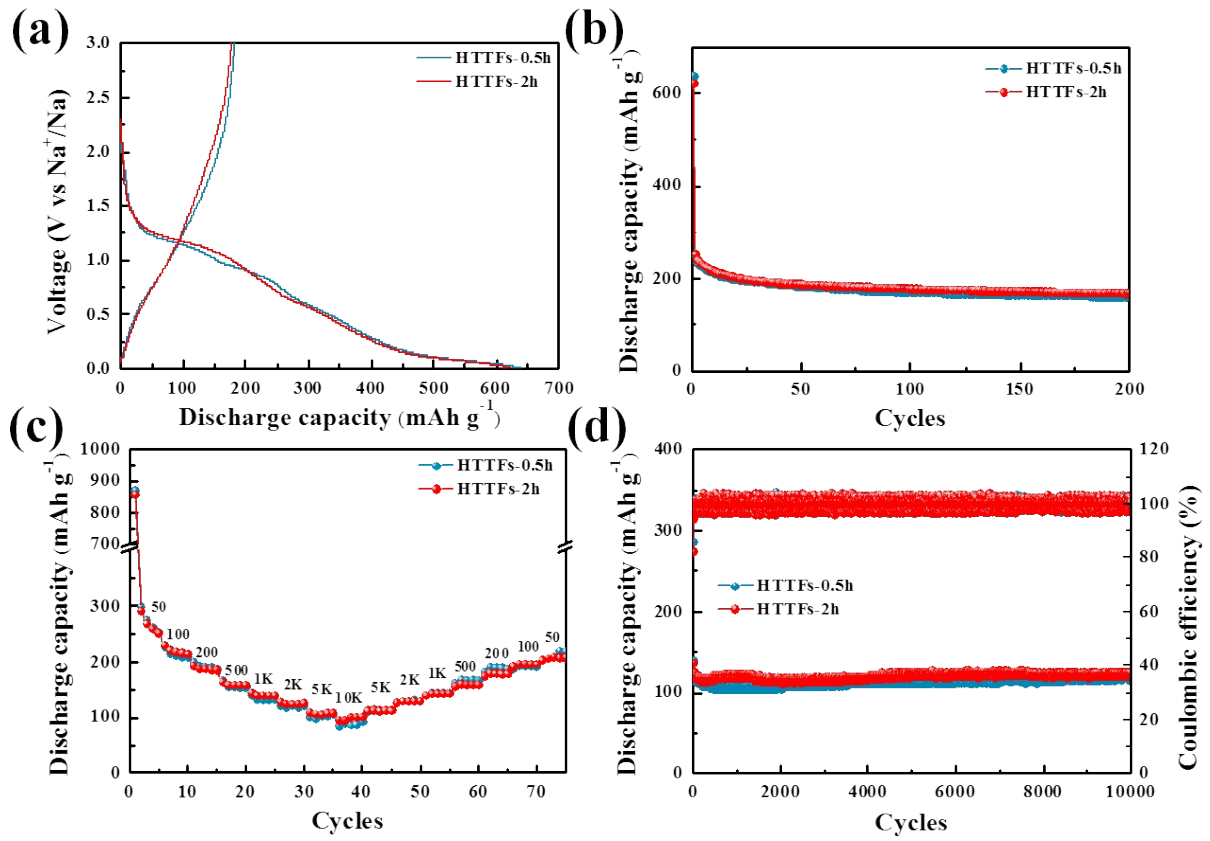

Fig. S7 (a) Charge/discharge profiles of HTTFs-0.5h and HTTFs-2h at 200 mA g^{-1}. (b) Cycling performance of HTTFs-0.5h and HTTFs-2h at 200 mA g^{-1} for 200 cycles. (d) Rate performance of HTTFs-0.5h and HTTFs-2h at different current densities. (e) Cycling performance of HTTFs-0.5h and HTTFs-2h at 5, 000 mA g^{-1} for 10, 000 cycles.

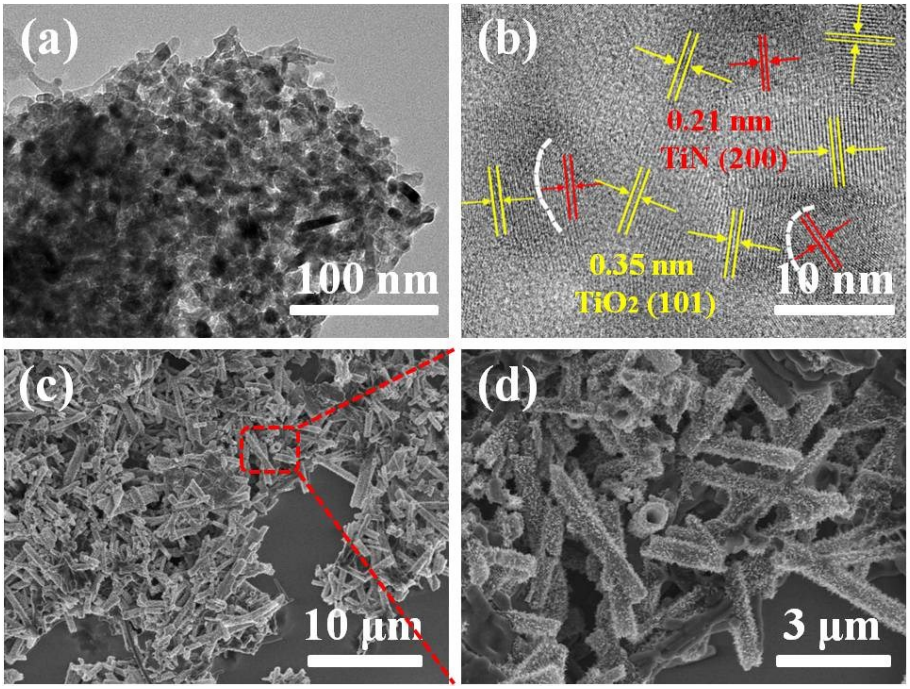

Fig. S8 (a) Low- and (b) high-magnification TEM and (c) low- and (d) high-magnification SEM images of the HTTFs-1h electrode after 1, 000 cycles at 5, 000 mA g^{-1}.

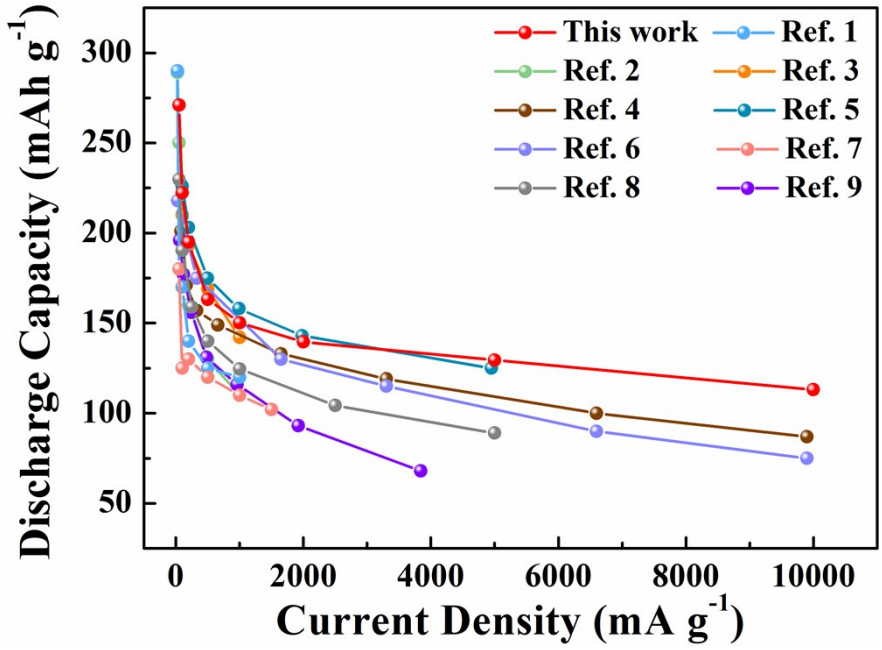

Fig. S9 Comparison of the rate capability of HTTFs-1h with previously reported TiO_2-based composites with various modification methods (reference numbers in supplementary table 3).

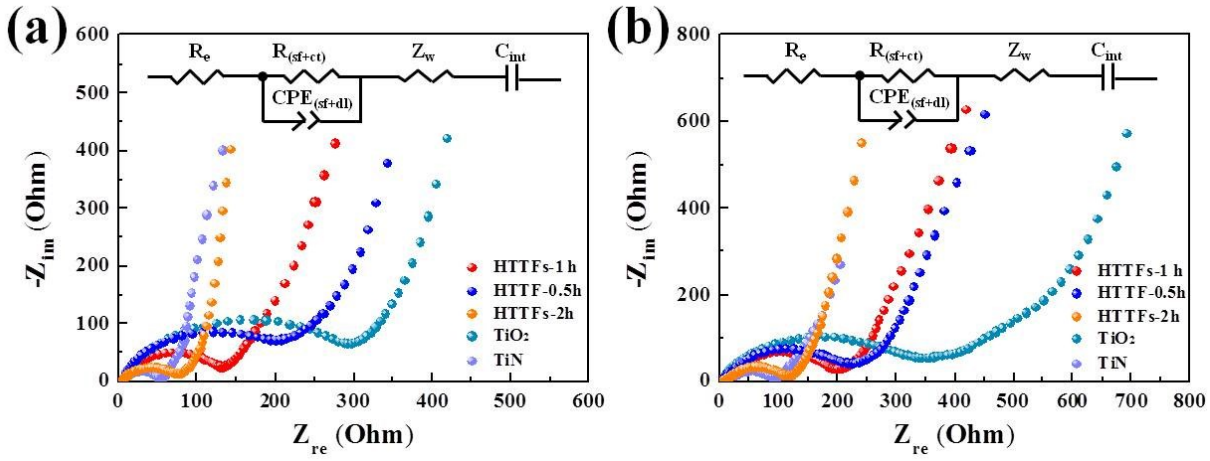

Fig. S10 EIS curves of the HTTFs-0.5h, HTTFs-1h, HTTFs-2h, pure TiN, and TiO_2 anodes (a) as-prepared electrodes and (b) electrodes after 1, 000 cycles at 5, 000 mA g^{-1}.

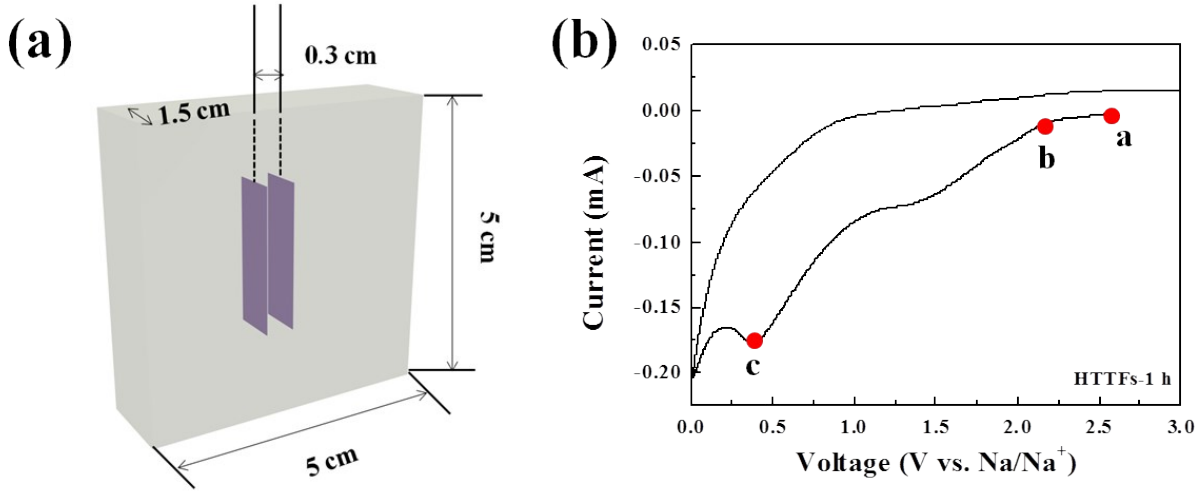

Fig. S11 (a) Schematic representation of the transparent testing cell. (b) Cyclic voltammogram for HTTFs-1h in a transparent mold at a scan rate of 5 mV s^{-1}.

Table S1. O and N element content statistics of HTTFs-1h.

Element	[norm. wt.%]	[norm. at.%]
N	1.5	2.78
O	40.7	65.93

Table S2. Nitrogen Brunauer–Emmett–Teller (BET) adsorption was performed to characterize the specific surface area, pore volume and pore-size distribution of pure TiO_2, HTTFs-0.5h, HTTFs-1h, HTTFs-2h and pure TiN samples.

BET			
Sample	**Surface Area m^2 g**	**Pore Diameter Dv(d) nm**	**Pore Volume cc g^{-1}**
HTTFs-0.5h	47.81	45.68	1.113961
HTTFs-1h	56.18	29.13	0.830718
HTTFs-2h	61.78	29.23	0.900487
pure TiO_2	47.10	29.52	0.706002
pure TiN	45.20	45.86	1.043999

Table S3. Cycling stability and rate capability comparison of HTTFs-1h versus reported TiO_2 anode materials in SIBs.

Materials	High rate capacity	Cycling performance	Ref.
Anatase-bronze hybrid TiO_2 nanosheets	290 mAh g^{-1} at 25 mA g^{-1}, 120 mAh g^{-1} at 1, 000 mA g^{-1}	120 mAh g^{-1} at 500 mA g^{-1} after 2, 500 cycles	[1]
Dual-phase hierarchical TiO_2 nanosheets	289 mAh g^{-1} at 25 mA g^{-1}, 110 mAh g^{-1} at 1, 000 mA g^{-1}	207 mAh g^{-1} at 100 mA g^{-1} after 100 cycles	[2]
Anatase TiO_2 nanotubes	210 mAh g^{-1} at 100 mA g^{-1}, 142 mAh g^{-1} at 1, 000 mA g^{-1}	132 mAh g^{-1} at 1, 000 mA g^{-1} after 250 cycles	[3]
TiO_2∩NPCSs	201 mAh g^{-1} at 82.5 mA g^{-1}, 87 mAh g^{-1} at 9, 900 mA g^{-1}	152 mAh g^{-1} at 660 mA g^{-1} after 3, 000 cycles	[4]
Co, N double-doped mesoporous TiO_2/C frameworks	226 mAh g^{-1} at 99 mA g^{-1}, 125 mAh g^{-1} at 4, 950 mA g^{-1}	100 mAh g^{-1} at 4, 950 mA g^{-1} after 10, 000 cycles	[5]
Anatase/bronze TiO_2 microsphere	218 mAh g^{-1} at 33 mA g^{-1}, 75 mAh g^{-1} at 9, 000 mA g^{-1}	125 mAh g^{-1} at 3, 300 mA g^{-1} after 1, 000 cycles	[6]
Anatase TiO_2	180 mAh g^{-1} at 50 mA g^{-1}, 102 mAh g^{-1} at 1, 500 mA g^{-1}	98 mAh g^{-1} at 500 mA g^{-1} after 1, 400 cycles	[7]
Oxygen-deficient anatase TiO_2 nanotubes (wires)/reduced graphene oxide (rGO) composites	229.7 mAh g^{-1} at 50 mA g^{-1}, 89 mAh g^{-1} at 5, 000 mA g^{-1}	134 mAh g^{-1} at 500 mA g^{-1} after 1, 000 cycles	[8]
TiO_2@$Ti_3C_2T_x$	218 mAh g^{-1} at 30 mA g^{-1}, 68 mAh g^{-1} at 3840 mA g^{-1}	110 mAh g^{-1} at 960 mA g^{-1} after 5, 000 cycles	[9]
HTTFs-1h	270.9 mAh g^{-1} at 50 mA g^{-1}, 113.1 mAh g^{-1} at 10, 000 mA g^{-1}	132.5 mAh g^{-1} at 5, 000 mA g^{-1} after 10, 000 cycles	This work

Table S4. Electrical parameters of the as-prepared electrodes and electrodes after 1, 000 cycles , determined from the fitting results of the impedance spectra data presented in Figure S10.

		Fitting results				
		pure TiO_2	**pure TiN**	**HTTFs-0.5h**	**HTTFs-1h**	**HTTFs-2h**
Before cycle	**R_{sf+ct} (ohm)**	281.9	47.12	206	124.9	73.64
After 1, 000 cycles	R_{sf+ct} (ohm)	321.1	95.59	234.2	208.7	124.5

References

1 R. R. Maça, C. J. Daniel, C. R. Miguel and V. Etacheri, *Chem. Eng. J.*, 2020, **391**, 123598.

2 W. L. Feng, R. R. Maca and V. Etacheri, *ACS Appl. Mater. Interfaces*, 2020, **12**, 4443-4453.

3 G. Cha, S. Mohajernia, N. T. Nguyen, A. Mazare, N. Denisov, I. Hwang and P. Schmuki, *Adv. Energy Mater.*, 2019, **10**, 1903448.

4 B. Li, B. Xi, F. Wu, H. Mao, J. Liu, J. Feng and S. Xiong, *Adv. Energy Mater.*, 2019, **9**, 1803070.

5 H. Xu, Y. T. Liu, T. T. Qiang, L. G. Qin, J. Chen, P. G. Zhang, Y. Zhang, W. Zhang, W. B. Tian and Z. M. Sun, *Energy Storage Materials*, 2019, **17**, 126-135.

6 J.-Y. Hwang, H.-L. Du, B.-N. Yun, M.-G. Jeong, J.-S. Kim, H. Kim, H.-G. Jung and Y.-K. Sun, *ACS Energy Lett.*, 2019, **4**, 494-501.

7 X. H. Wang, L. Qi and H. Y. Wang, *ACS Appl. Mater. Interfaces*, 2019, **11**, 30453-30459.

8 W. G. Wang, M. Wu, P. Han, Y. Liu, L. He, Q. H. Huang, J. Wang, W. S. Yan, L. J. Fu and Y. P. Wu, *ACS Appl. Mater. Interfaces*, 2019, **11**, 3061-3069.

9 X. Guo, J. Q. Zhang, J. J. Song, W. J. Wu, H. Liu, and G. X. Wang, *Energy Storage Mater.*, 2018, **14**, 306-313.